RalA and the exocyst complex influence neuronal polarity through PAR-3 and aPKC

Giovanna Lalli

The Wolfson Centre for Age-Related Diseases, King's College London, London SE1 1UL, UK
e-mail: giovanna.lalli@kcl.ac.uk

Accepted 9 February 2009
Journal of Cell Science 122, 1499-1506 Published by The Company of Biologists 2009
doi:10.1242/jcs.044339

Summary

Neuronal polarization requires localized cytoskeletal changes and polarized membrane traffic. Here, I report that the small GTPase RalA, previously shown to control neurite branching, also regulates neuronal polarity. RalA depletion, or ectopic expression of constitutively active RalA in cultured neurons inhibit axon formation. However, expression of a constitutively active RalA mutant that is unable to interact with the exocyst complex has no effect on neuronal polarization. Furthermore, depletion of the Sec6, Sec8 or Exo84 subunits of the exocyst complex also leads to unpolarized neurons. Early stages of neuronal polarization are accompanied by increasing levels of interaction of the exocyst complex with PAR-3 and atypical protein kinase C (aPKC), and by the RalA-dependent association of the exocyst complex with PAR-3. Thus, neuronal polarization involves a RalA-regulated association between mediators of vesicle trafficking (exocyst complex) and cell polarity (PAR-3).

Supplementary material available online at
http://jcs.biologists.org/cgi/content/full/122/10/1499/DC1

Key words: Ral, Neuronal polarity, Exocyst, PAR-3, aPKC

Introduction

The ability of a cell to acquire a highly polarized morphology is crucial for complex biological activities, such as the organization of the nervous system. Several signalling pathways have been shown to control neuronal polarization in vitro and in vivo (Arimura and Kaibuchi, 2007; Barnes et al., 2008). Among the key regulators of this event is the partitioning defect (PAR) PAR-3/PAR-6/aPKC complex (Goldstein and Macara, 2007). During the in vitro polarization of hippocampal neurons (Dotti et al., 1988), the PAR/aPKC complex becomes concentrated from multiple minor neurites extending from the neuronal cell body (stage 2) into the tip of the single developing future axon (stage 3) (Arimura and Kaibuchi, 2007). The proper localization of the PAR/aPKC complex is necessary for neuronal polarization through its influence on the actin and microtubule cytoskeleton (Chen et al., 2006; Nishimura et al., 2005).

Neuronal polarity relies on coordinated cytoskeletal rearrangements and directed membrane traffic. Indeed, polarized membrane transport can already be observed in stage 2 neurons before axon extension (Bradke and Dotti, 1997; Calderon de Anda et al., 2008). Axon specification is therefore likely to involve spatial regulation of membrane delivery. The exocyst, an evolutionarily conserved octameric complex (Sec3, Sec5, Sec6, Sec8, Sec10, Sec15, Exo70 and Exo84) (Hsu et al., 1998) tethers secretory vesicles to specific domains of the plasma membrane, particularly in regions of polarized exocytosis, such as the growing bud in the yeast *Saccharomyces cerevisiae* (Zhang et al., 2005) and the basolateral membrane in epithelial cells (Grindstaff et al., 1998; Langevin et al., 2005). In neurons, members of the exocyst complex contribute to neurite outgrowth and receptor transport to the synapse (Mehta et al., 2005; Sans et al., 2003; Vega and Hsu, 2001). However, the role of exocyst components in the establishment of neuronal polarity in mammalian systems has not yet been investigated. In mammals, the exocyst complex acts as an effector of the Ras-like (Ral) GTPase isoforms RalA and RalB (Moskalenko et al., 2002), mediating a variety of cellular processes, including filopodia formation (Sugihara et al., 2002) and cell migration (Rosse et al., 2006). In neurons, I have previously shown that the exocyst participates in neurite branching downstream of integrin and Ral signalling (Lalli and Hall, 2005). However, the potential function of Ral and the exocyst in axon specification remains unknown. In this report, I show that RalA influences neuronal polarity through the exocyst complex and the polarity proteins PAR-3 and aPKC.

Results and Discussion

RalA is involved in neuronal polarization

Ral has been previously shown to regulate neurite branching (Lalli and Hall, 2005). To analyze the role of Ral in more detail at earlier developmental stages, cultured cortical neurons were examined in the initial phases of their development in vitro. Forty-eight hours after plating, 75% of neurons polarize and extend a single process positive for the axonal marker tau-1 (data not shown). Depletion of endogenous RalA by nucleofection with small interfering (si)RNA oligonucleotides caused a twofold increase in the number of unpolarized cells, which showed multiple tau-1-negative minor neurites (Fig. 1A,B, left graph). This was accompanied by a threefold increase in neurite length (Fig. 1B, middle graph). RNA interference (RNAi)-mediated depletion of RalB had no significant effect on neuronal polarization (data not shown). Consistent with previous data, in RalA-depleted neurons that did polarize, the branch density of axons was lower, but the branch density of minor neurites (not previously examined) was largely unaffected (supplementary material Fig. S1A-D). The partial inhibition of neuronal polarity is probably due to the time interval necessary for RNAi-mediated RalA protein depletion. Overall, these results indicate that RalA is involved in axon development, as well as axon branching, a dual function observed also for other proteins, such as c-Jun N-terminal

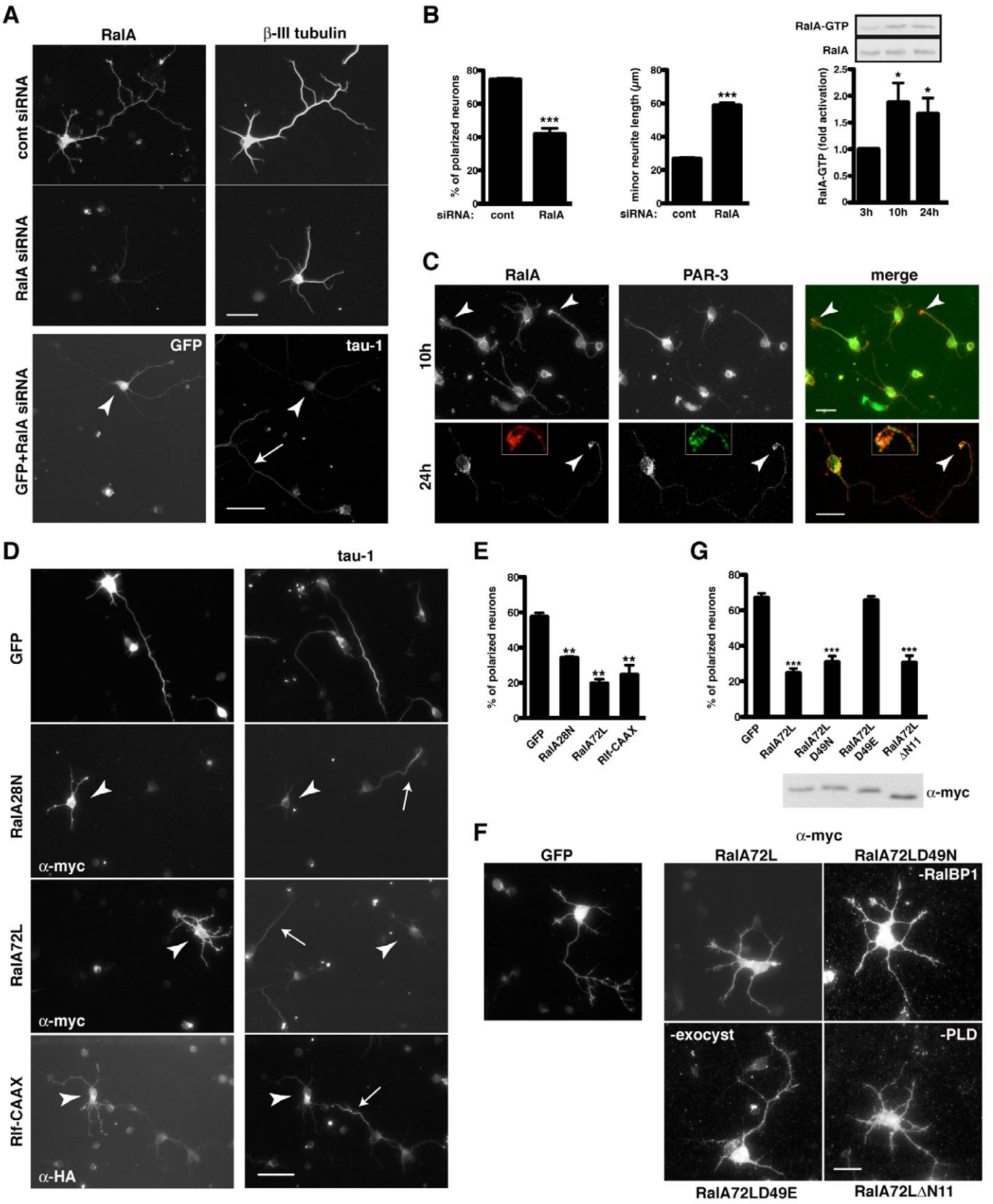

Fig. 1. See next page for legend.

Fig. 1. RalA is required for neuronal polarity. (A) Cortical neurons stained for RalA and neuron-specific β-III tubulin 48 hours after nucleofection of control (top) or RalA siRNA (centre). Control cells positive for RalA display a polarized morphology, whereas a considerable portion of RalA-depleted cells lacks a major process. These RalA-depleted cells (visualized by co-transfection of GFP with RalA siRNA) are not polarized, as shown by lack of tau-1 staining (bottom, arrowhead). The arrow indicates a tau-1-positive axon of an untransfected cell. Scale bars: 40 µm. (B) (Left) Quantification of polarization in cortical neurons 48 hours after nucleofection of control or RalA siRNA (mean ± s.e.m.: control siRNA, 74.53±0.87; RalA siRNA, 41.77±3.53; ***P<0.001). (Centre) Quantification of minor neurite length in control and RalA siRNA (mean ± s.e.m.: control siRNA, 26.80±0.87; RalA siRNA, 58.70±1.70; ***P<0.001). (Right) Active RalA levels increase at early stages of polarization. Neurons were lysed at the indicated time points after plating and assayed for active RalA levels by a Ral-GTP pull down. A representative blot is shown (top), together with data quantification (bottom; mean ± s.e.m.: 10 hours, 1.88±0.36; 24 hours, 1.66±0.29; *P<0.05). (C) At early stages of neuronal polarization (10 hours), RalA concentrates in one emerging neurite tip before PAR-3 (top row, arrowheads). Partial colocalization of RalA with PAR-3 at axon tips shown by a confocal section of a polarized neuron at later times (24 hours) (bottom row, arrowheads). Insets show a magnification of the axon growth cone. Scale bars: 20 µm. (D) Cortical neurons nucleofected with GFP, myc-tagged dominant-negative (RalA28N) or constitutively active (RalA72L) RalA, or an HA-tagged constitutively active RalGEF (Rlf-CAAX) stained with anti-myc or anti-HA and anti-tau-1 (right) antibodies 24 hours after plating. GFP-expressing neurons have a tau-1-positive axon (top row), whereas many cells transfected with Ral mutants or Rlf-CAAX lack tau-1 staining (arrowheads). Arrows indicate tau-1-positive axons of untransfected cells. Scale bar: 40 µm. (E) Quantification of the neuronal polarity defect (mean ± s.e.m.: GFP, 57.47±2.22; RalA28N, 34.23±0.67; RalA72L, 19.6±2.46; Rlf-CAAX, 24.53±5.42; **P<0.01). (F) Cortical neurons nucleofected with GFP or the indicated myc-tagged RalA constructs stained with anti-myc antibody 24 hours after nucleofection. Cells expressing constitutively active RalA (RalA72L) show an unpolarized phenotype also observed in cells expressing the active RalA mutants unable to interact with RalBP1 (RalA72LD49N) or with PLD (RalA72LΔN11). By contrast, neurons expressing the active RalA mutant unable to interact with the exocyst complex (RalA72LD49E) display a polarized morphology. Scale bar: 20 µm. (G) (Top) Quantification of the polarity defect in neurons expressing the indicated constructs (mean ± s.e.m.: GFP, 67.12±2.36; RalA72L, 24.63±2.57; RalA72LD49N, 30.83±3.43; RalA72LD49E, 65.6±2.20; RalA72LΔN11, 30.55±3.89; ***P<0.001). (Bottom) Western blot analysis shows similar expression levels of the myc-tagged RalA constructs.

kinase (JNK)-interacting protein 1 (JIP1) (Dajas-Bailador et al., 2008).

To determine the activity of endogenous RalA during neuronal polarization, a Ral-GTP pull-down assay was used (Tian et al., 2002). RalA activity increased after plating and peaked at 10 hours, at early stages of polarization, remaining at similar levels at 24 hours (Fig. 1B, right graph). The cellular distribution of RalA during neuronal polarization was visualized, together with PAR-3, at different times after plating. Neurons were categorized by the criteria proposed by Dotti (Dotti et al., 1988): after the initial sprouting of two neurites from opposite poles of the cell body, stage 2 neurons develop multiple neurites, whereas, by stage 3, one neurite – preferably one of the initial two sprouting processes (Calderon de Anda et al., 2008) – has become longer and begun to acquire axonal characteristics. RalA was found to concentrate at the tips of the longest extending neurite as early as 10 hours after plating (beginning of stage 3), before a clear accumulation of PAR-3 could be detected (Fig. 1C, top row, arrowheads), whereas partial colocalization between RalA and PAR-3 could be observed 24 hours after plating (Fig. 1C, bottom row, arrowheads). The accumulation of RalA at the emerging axon tip in stage 3 neurons was quantitatively confirmed by ratiometric imaging against the cytoplasmic tracer 5-chloromethylfluoresceine diacetate (CMFDA) fluorescence (Nishimura et al., 2004) (supplementary material Fig. S1E, right graph). Together, these data indicate that spatial accumulation and temporal activation of RalA occur during early phases of axon specification.

To further investigate the role of RalA during polarization, cortical neurons were nucleofected before plating with myc-tagged constitutively active (RalA72L) or dominant-negative (RalA28N) versions of RalA, or with HA-tagged Rlf-CAAX, a constitutively active Ral guanine nucleotide exchange factor (GEF) (Lalli and Hall, 2005). Cells were fixed 24 hours later and co-stained for tau-1. Compared with GFP-expressing control cells, all three plasmids induced neurons with multiple tau-1-negative neurites (Fig. 1D, arrowheads). Quantification showed a twofold reduction of polarized neurons (Fig. 1E). These results support the involvement of RalA in the establishment of neuronal polarity. The fact that either inactivation or global activation of RalA impaired axon formation indicates that a tight spatial and temporal regulation of Ral activity is needed for axon specification, a requirement essential also for other cellular roles of Ral (Moskalenko et al., 2002; Ward et al., 2001). In addition, cycling of RalA between the GDP- and the GTP-bound forms could be essential for its function in neuronal polarity, similar to Cdc42 (Schwamborn and Puschel, 2004). To test this hypothesis, the effect of a myc-tagged 'fast-cycling' RalA mutant (RalAF39L) (Omidvar et al., 2006) on neuronal polarization was examined. Nucleofection of this mutant proved detrimental to neurons, which exhibited substantial neurite blebbing. However, cells expressing low amounts of RalAF39L extended multiple tau-1-positive neurites longer than normal minor neurites (data not shown), suggesting that RalA cycling is indeed required for proper neuronal polarization.

RalA influences neuronal polarity through the exocyst complex

To determine which RalA effector (target) proteins contribute to neuronal polarity, myc-tagged constitutively active RalA (RalA72L) constructs harbouring additional mutations were used. Previous work identified distinct loss of binding of RalA72LD49N to RalBP1, RalA72LD49E to the exocyst complex and RalA72LΔN11 to phospholipase D (PLD) (Lalli and Hall, 2005). Neurons were nucleofected before plating, then fixed and co-stained for tau-1 24 hours later to quantify the effect on neuronal polarization. Importantly, all the active RalA mutants induced an unpolarized phenotype similar to the one observed with active RalA72L except for RalA72LD49E, the mutant unable to interact with the exocyst (Fig. 1F,G). These data strongly support a specific role for the exocyst complex among different Ral effectors in neuronal polarization.

The exocyst complex is essential for neuronal polarization

To investigate the role of the exocyst in neuronal polarization, the morphology of cortical neurons depleted of endogenous exocyst components by RNAi was assessed 48 hours after siRNA nucleofection. Three exocyst components (Sec6, Sec8 and Exo84) implicated in morphological differentiation or essential for the organization of a functional exocyst complex were targeted (Anitei et al., 2006; Blankenship et al., 2007; Zhang et al., 2005). Cells almost completely depleted of Sec6, Sec8 or Exo84, as judged by immunofluorescence, were found to be unpolarized, showing long tau-1-negative neurites emerging from the cell body (Fig. 2A,B). A fraction of depleted neurons still displayed a polarized morphology, though these did have a modest decrease in neurite

length and a more substantial decrease in both minor neurite and axon branch density (supplementary material Fig. S2A-C), consistent with the reported role for the exocyst complex in branching (Lalli and Hall, 2005). Quantification showed that RNAi of the different exocyst subunits caused a greater than 60% decrease in polarized neurons (Fig. 2C). Interestingly, even though there was a general expected decrease in total neurite length compared with control cells, neurites extending from the cell body were considerably longer than average minor neurites of control cells, as observed in neurons depleted of PAR-3 (Schwamborn et al., 2007)

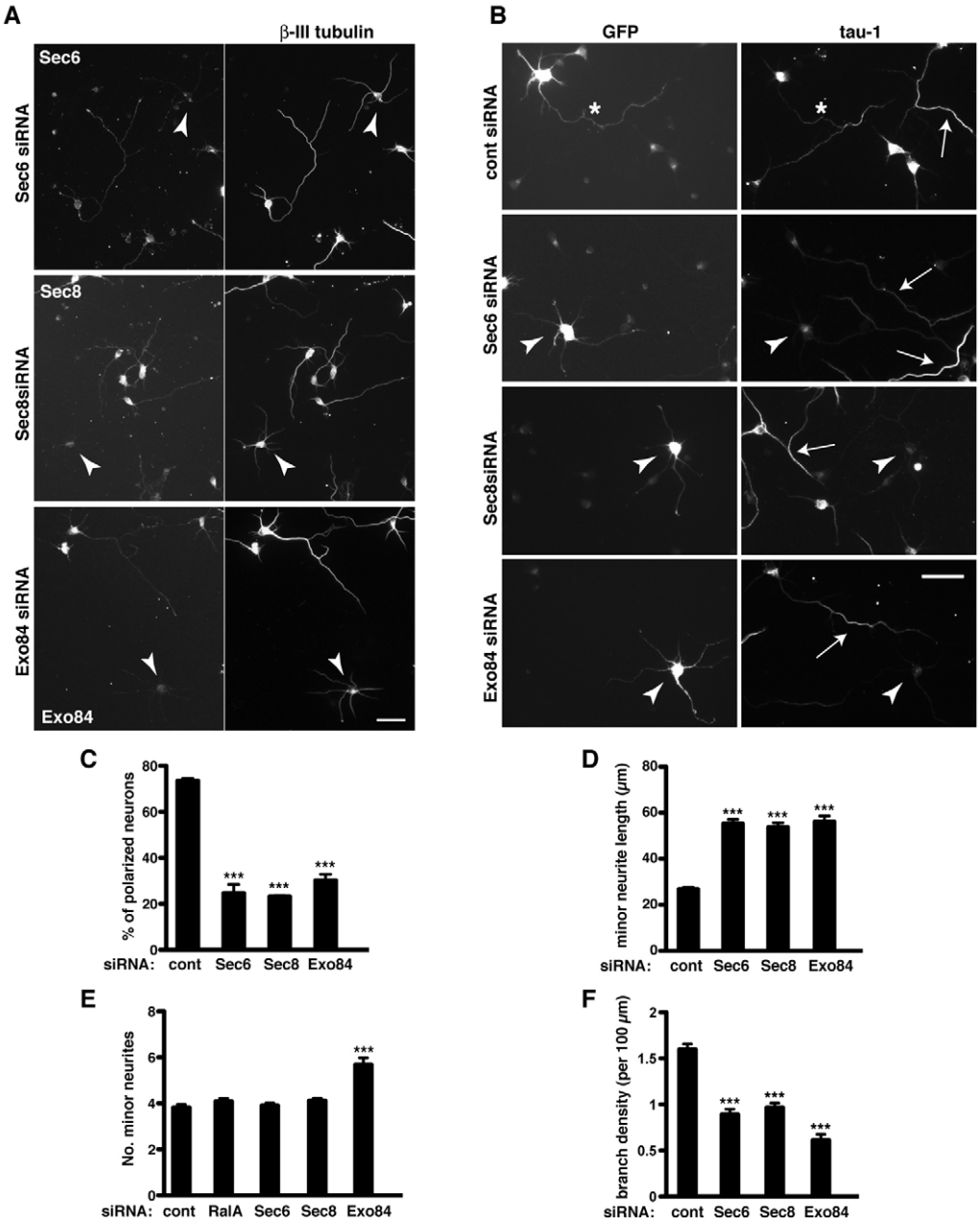

Fig. 2. Cortical neurons lacking exocyst subunits are unpolarized. (A) Cortical neurons nucleofected with the indicated siRNA and co-stained for the indicated exocyst subunits and β-III tubulin 48 hours after plating. Cells depleted of Sec6, Sec8 or Exo84 lack a major process (arrowheads). Cells retaining exocyst subunits in the same field are shown as a staining control. (B) Neurons nucleofected with the indicated siRNA plus GFP stained for tau-1 48 hours after plating. Control cells show a tau-1-positive axon (asterisk), whereas cells lacking exocyst subunits display multiple tau-1-negative neurites (arrowheads). Arrows indicate tau-1-positive axons of untransfected cells. Scale bars: 40 μm. (C) Quantification of the neuronal polarity defect in cells lacking the indicated exocyst subunits (mean ± s.e.m.: control siRNA, 73.5±1.01; Sec6 siRNA, 24.62±3.79; Sec8 siRNA, 23.17±0.37; Exo84 siRNA, 30.18±2.68; ***P<0.001). (D) Depletion of exocyst subunits increases the length of the tau-1-negative minor neurites (mean ± s.e.m.: control siRNA, 26.80±0.87; Sec6 siRNA, 55.32±1.78; Sec8 siRNA, 53.77±1.87; Exo84 siRNA, 56.15±2.49; ***P<0.001). (E) The number of minor neurites emerging from the cell body increases only in Exo84-depleted neurons (mean ± s.e.m.: control siRNA, 3.82±0.13; RalA siRNA, 4.09±0.13; Sec6 siRNA, 3.90±0.11; Sec8 siRNA, 4.12±0.11; Exo84 siRNA, 5.68±0.30; ***P<0.001). (F) Depletion of exocyst subunits decreases total branch density (mean ± s.e.m.: control siRNA, 1.60±0.06; Sec6 siRNA, 0.89±0.06; Sec8 siRNA, 0.96±0.05; Exo84 siRNA, 0.61±0.06; ***P<0.001).

or RalA (Fig. 2D, compare with Fig. 1B, middle graph). The latter observation is consistent with previous studies showing that RalA depletion destabilizes exocyst complex formation (Moskalenko et al., 2002). Depletion of exocyst subunits had a more severe effect on polarization compared with RalA knockdown. This might be due to different efficiency of the RNAi approach in achieving sufficient depletion of these proteins in early polarization stages. Alternatively, the exocyst complex might also act via other RalA-independent polarization signalling pathways. Strikingly, only Exo84 RNAi caused a significant increase of the total number of

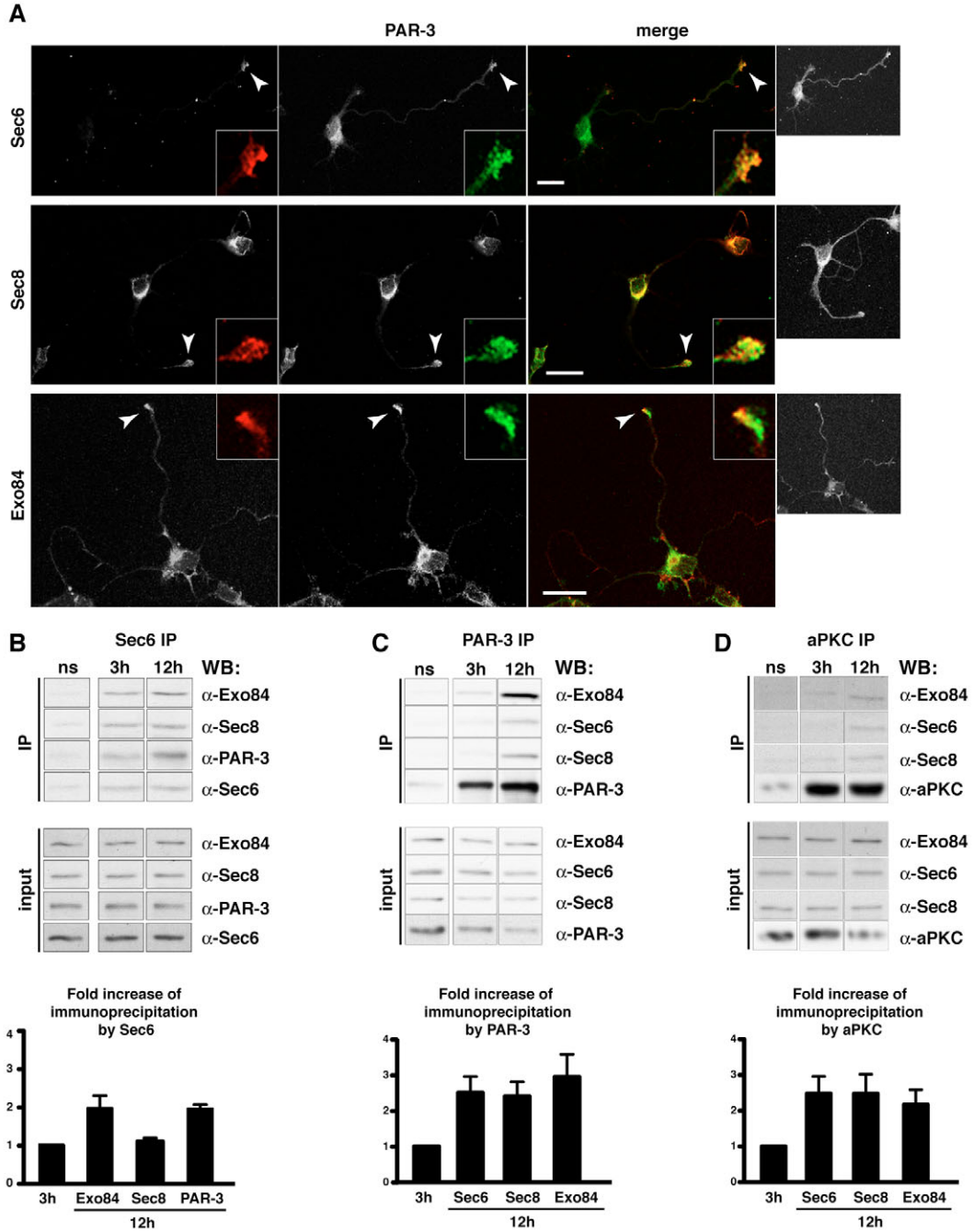

Fig. 3. The exocyst complex interacts with PAR-3 and aPKC during neuronal polarization. (A) Confocal sections of neurons showing colocalization of Sec6, Sec8 and Exo84 with PAR-3 at the tips of emerging axons (arrowheads). Insets show a magnification of the axon growth cones. Panels on the right are projections of the confocal sections and show total neuronal morphology. Scale bars: 20 μm. (B) Gradual assembly of the exocyst complex assessed by co-IP of endogenous Sec8 and Exo84 using an anti-Sec6 antibody at the indicated times after plating. Endogenous Sec8 is immunoprecipitated in similar amounts throughout the analyzed time interval, whereas Exo84 and PAR-3 are precipitated in increasing amounts with time (top panel and graph). Quantification of fold increase in the interaction of Sec6 with the indicated proteins at 12 hours was calculated relative to 3 hours and normalized to the amount of correspondent protein in lysates (mean ± s.e.m.: Exo84, 1.96c0.32; Sec8, 1.11±0.09; PAR-3, 1.97±0.10). (C) Sec6, Sec8 and Exo84 co-immunoprecipitate with PAR-3 during neuronal polarization. The PAR-3-exocyst subunit interaction increases from 3 hours to 12 hours (bottom graph, mean ± s.e.m.: Sec6, 2.50±0.45; Sec8, 2.40±0.41; Exo84, 2.94±0.63). (D) Sec6, Sec8 and Exo84 co-immunoprecipitate with aPKC during neuronal polarization (top panel). The aPKC-exocyst subunit interaction increases from 3 hours to 12 hours (bottom graph, mean ± s.e.m.: Sec6, 2.48±0.48; Sec8, 2.48±0.54; Exo84, 2.16±0.41). ns lanes, negative control IP with a non-specific antibody.

neurites in unpolarized neurons (Fig. 2E). As the efficiency of knockdown was comparable for all the targeted exocyst subunits as shown by western blot analysis (supplementary material Fig. S3), this result suggests that Exo84 might have additional specific functions in neuronal polarization, consistent with its role in promoting epithelial apical identity in *Drosophila* (Blankenship et al., 2007). Finally, unpolarized cells lacking exocyst subunits also had a less complex morphology, owing to decreased total branch density (Fig. 2F). Taken together, these results strongly support a dual role for the exocyst complex in neurite branching and neuronal polarity.

PAR-3 and aPKC interact with the exocyst during neuronal polarization

To analyze the localization of Sec6, Sec8 and Exo84 during neuronal polarization, cortical neurons were immunostained at different times after plating. All three proteins displayed a punctate, uniform distribution at stage 2 (data not shown). However, at stage 3 the exocyst subunits appeared concentrated at the tip of the presumptive axonal process, where they colocalized with PAR-3 (Fig. 3A, arrowheads). Quantitative ratiometric fluorescence/CMFDA analysis confirmed accumulation at the axon tip for Sec6 and Exo84, but not for Sec8 (supplementary material Fig. S1E). The failure to detect

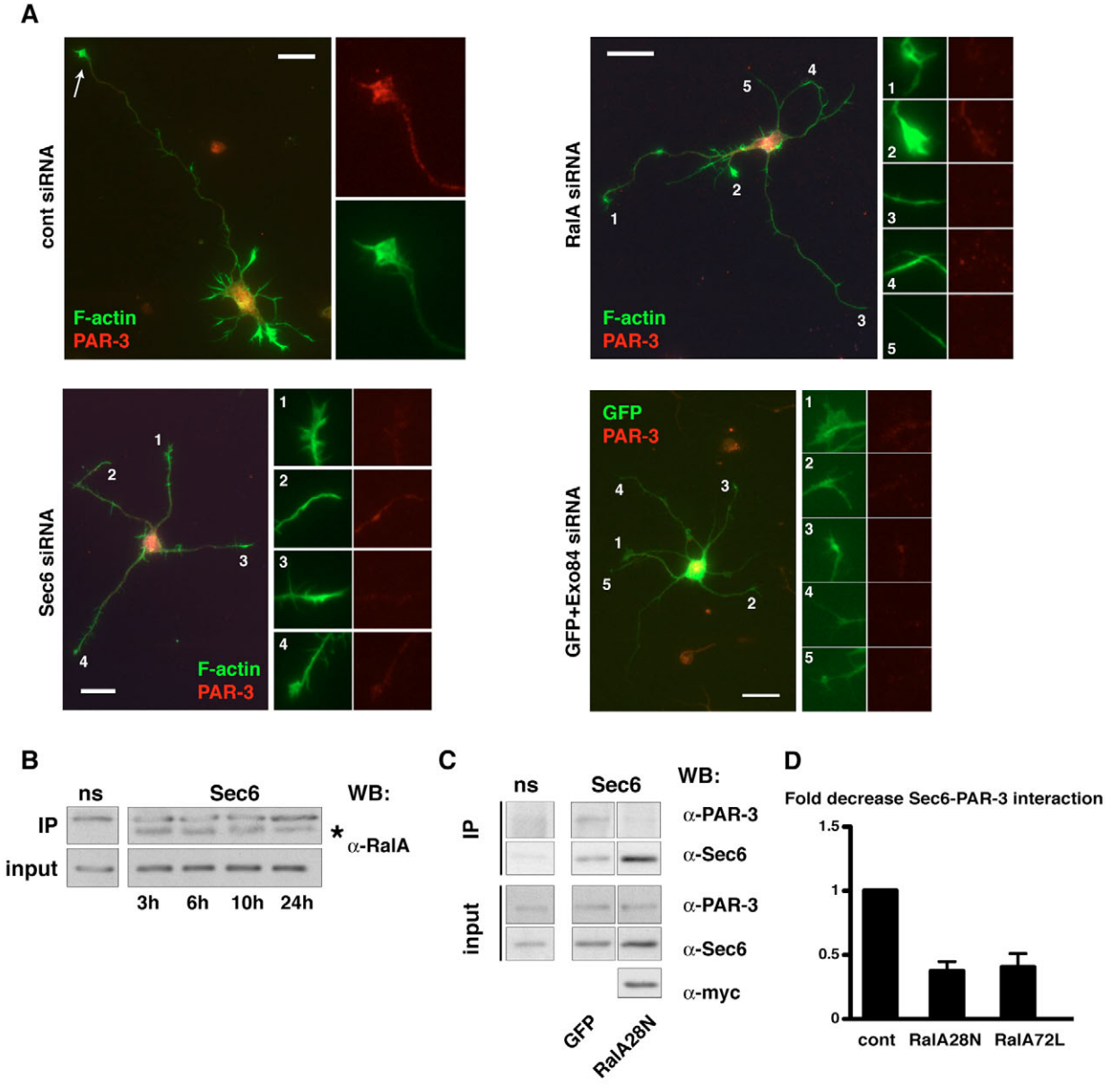

Fig. 4. RalA regulates the interaction of PAR-3 with the exocyst. (A) Cortical neurons nucleofected with the indicated siRNA, fixed 48 hours after plating and stained for PAR-3, the protein of interest (RalA, Sec6 or Sec8, data not shown) or co-transfected GFP in the case of Exo84 siRNA and F-actin to visualize neuronal morphology. In control cells, PAR-3 accumulates at the axonal tip (top left). Unpolarized neurons lacking RalA (top right), Sec6 (bottom left) or Exo84 (bottom right) show a faint diffuse PAR-3 staining. Insets show a magnification of the numbered growth cones. Scale bars: 20 μm. (B) RalA co-immunoprecipitates with Sec6 at different time points during neuronal polarization. Asterisk indicates the RalA band visible under the light chain of the anti-Sec6 antibody used for the IP. The RalA band is not present in a control IP with a non-specific antibody (ns lane). (C) Cortical neurons were nucleofected with GFP or myc-tagged RalA28N. IP with an anti-Sec6 antibody was carried out 24 hours after plating. Co-IP of PAR-3 is significantly decreased in neurons transfected with RalA28N. ns lane, negative control IP with a non-specific antibody. (D) Quantification of fold decrease in Sec6-PAR-3 interaction in RalA28N or RalA72L-nucleofected neurons compared with GFP-transfected cells (mean ± s.e.m.: RalA28N, 0.37±0.07; RalA72L, 0.40±0.10).

accumulation of Sec8 could be due to a more transient, and therefore less detectable, accumulation of this protein at the axon growth cone. If the exocyst indeed participates in neuronal polarization, it might be expected that the complex would assemble during early stages of neuronal development. Under the culture conditions used, polarization occurs between 10 and 24 hours after plating, with over 60% of neurons having a tau-1-positive axon at 24 hours (data not shown). Mammalian exocyst components can be found as distinct subcomplexes on vesicles (Sec10, Sec15, Exo84) and on the plasma membrane (Sec3, Sec5, Sec6, Sec8, Exo70) (Moskalenko et al., 2003). Complex assembly can therefore be monitored by examining the presence of a component of one subcomplex in immunoprecipitates of a component from the other subcomplex. Whereas the association of Sec6 with Sec8 (same subcomplex) remained constant from 3 to 12 hours after plating, the interaction between Sec6 and Exo84 (different subcomplexes) increased with time (Fig. 3B). Interestingly, Sec6 immunoprecipitates also contained increasing levels of PAR-3, suggesting an association between this polarity protein and the exocyst complex (Fig. 3B). Further studies will be needed to fully clarify the molecular nature of such an interaction.

To further confirm the association of the exocyst complex with PAR-3, an anti-PAR-3 antibody was used for immunoprecipitation (IP), and an increasing interaction with Exo84, Sec8 and Sec6 could be detected from 3 to 12 hours (Fig. 3C). Finally, an anti-aPKC antibody was also found to immunoprecipitate all three exocyst subunits (Fig. 3D). The interaction of aPKC with the exocyst components increased with time and correlated with an enhanced Sec6/Exo84 interaction. Taken together, these results strongly support a role for the exocyst complex in axon specification involving an interaction with PAR-3 and aPKC. The coordination between exocyst complex assembly and its interaction with PAR-3/aPKC could ensure the polarized membrane delivery essential for axon specification and growth, and has not been previously reported. Interestingly, in *S. cerevisiae*, the Par1 counterparts Kin1 and Kin2 show genetic interaction with multiple components of the exocyst complex, and have been implicated in the regulation of late stages of exocytosis and the establishment of cell polarity (Elbert et al., 2005).

RalA and the exocyst are essential for PAR-3 localization

The unpolarized phenotype observed in neurons lacking either RalA or exocyst complex subunits, together with the interaction between the exocyst and PAR-3/aPKC prompted an analysis of the localization of PAR-3 in RalA- and exocyst subunit-depleted neurons. As shown in Fig. 4A, PAR-3 did not accumulate in any of the neurites after RalA or exocyst subunit depletion. This strongly supports a role for RalA and the exocyst complex in neuronal polarity by contributing to the correct localization of PAR-3. RalA interacts with Sec5 and Exo84, and has been proposed to regulate the assembly of a full octameric exocyst complex (Moskalenko et al., 2003). In cortical neurons, RalA appears to constantly interact with Sec6 (Fig. 4B); however, its activity increases with time during polarization (Fig. 1B, left graph). RalA may therefore participate not only in the initial stages of neuronal polarization, but also in the later phase of axon extension, as it continues to be localized at axonal tips (Fig. 1C).

Finally, in order to determine whether RalA is required for the interaction of PAR-3 with the exocyst, dominant-negative or constitutively active RalA versions were transfected into cortical neurons. Consistent with the observed effects on neuronal morphology (Fig. 1D), both constructs substantially impaired the Sec6/PAR-3 interaction (Fig. 4C,D), indicating that RalA may regulate the exocyst/PAR-3 interaction. As the localization of RalA at the nascent axon tip correlates with the reported localization of Ras, Rap and Cdc42 (Arimura and Kaibuchi, 2007), these GTPases might function upstream of RalA as shown in other cellular contexts (Feig, 2003; Frische et al., 2007).

In conclusion, localized activation of RalA at early stages of polarization may ensure spatial regulation of the exocyst (Spiczka and Yeaman, 2008) and of PAR-3, highlighting the requirement of a functional secretory pathway for the correct positioning of cell polarity regulators. A local interaction of the PAR complex with the exocyst could therefore be important for the establishment and reinforcement of cell polarity during axon growth. It remains to be seen whether the PAR complex actively regulates polarized secretion, or whether the exocyst complex contributes to PAR-3 trafficking, for example by its previously reported interaction with Rab11 (Wu et al., 2005). Preferential assembly of the exocyst complex in the nascent axon favoured by RalA could also promote polarized membrane trafficking to the axon (Bradke and Dotti, 1997; Gartner et al., 2006). By revealing an unexpected link between RalA and the exocyst with the PAR-3/aPKC polarity complex, this study provides new insights into an important crosstalk between membrane traffic and cytoskeletal remodelling in neuronal polarization.

Materials and Methods

Reagents were obtained from Sigma unless otherwise specified. Antibodies used were: mouse anti-RalA, mouse anti-Sec8 and rabbit anti-β-actin (BD Biosciences); mouse or rabbit anti-myc and rabbit anti-β-III tubulin (Abcam); mouse anti-Sec6 and mouse anti-tau-1 (Calbiochem); mouse anti-Exo84 (a gift from Shu Hsu, Rutgers University, Piscataway, NJ); rabbit anti-PAR-3 (Upstate); and rabbit anti-aPKC (Santa Cruz and Zymed). Cell culture media, supplements, Alexa 488, Alexa 350 and Texas Red fluorescent secondary antibodies, Alexa 488 phalloidin and CMFDA were obtained from Invitrogen. Ral-GTP assay beads were purchased from Upstate.

Cell culture

Cortical neurons were prepared from E18 rat embryos, nucleofected (Amaxa) and plated on polyornithine-coated dishes or coverslips (Lalli and Hall, 2005). For Ral-GTP pull down assays, cells were plated on a 35 mm dish (1.5×10^6 cells/dish). For IP experiments, neurons were plated on 10 mm plastic dishes (6.5×10^6 cells/dish).

RNAi

Dissociated neurons were nucleofected with 9 μg of an siRNA duplex targeting RalA (Lalli and Hall, 2005) or a 'smart pool' of four siRNA duplexes targeting either Sec6, Sec8 or Exo84 (Thermo-Scientific/Dharmacon). As a control, equivalent amounts of a control siRNA duplex were used (MWG). Cells were immunostained or lysed 48 hours after siRNA nucleofection. In some experiments, GFP was co-nucleofected with siRNA at a 1:3 ratio.

Immunofluorescence and imaging analysis

Neurons were processed for immunofluorescence as described (Lalli and Hall, 2005). For Exo84, neurons could also be fixed in pre-chilled methanol 5 minutes at –20°C. After blocking, cells were incubated with primary antibodies overnight at 4°C in PBS containing 1% BSA and 0.25% gelatin (antibody buffer) followed by 25 minutes incubation with secondary antibodies diluted in antibody buffer. Images were captured with a Zeiss AxioCam MRm CCD digital camera connected to an inverted Axioplan 2 microscope equipped with the ApoTome system and 63× 1.4 NA, 40× 0.95 NA and 20× 0.75 NA Plan-Apochromat objectives (Carl Zeiss) using the Zeiss AxioVision 4.6 software. Confocal images were acquired with a Zeiss LSM 510 microscope equipped with a 40× 1.3 NA DIC Plan-Apochromat objective, using the 488 and 543 nm lines of a krypton-argon and helium-neon lasers, respectively. Images were collected by averaging eight times at a single focal plane. Sections along the *z*-axis were spaced at 0.4 μm intervals. Images were processed with Photoshop CS3 using the brightness/contrast adjustments applied to the entire pictures.

For neuronal polarity analysis, isolated neurons extending single processes that were at least twice as long as the other neurites and/or tau-1-positive were scored as polarized. Between 20 and 100 cells were analyzed per experiment, and the results of at least three independent experiments pooled for each condition. For neurite number, length and branch density measurements, 20 cells were analyzed per experiment and the results of at least three independent experiments pooled for each condition. Cell profiles were manually traced using NIH ImageJ. Only minor neurites

that were at least as long as the cell body diameter and branches greater than 10 μm were considered.

For fluorescence/CMFDA ratiometric analysis, neurons were incubated with 10 μM CellTracker green CMFDA for 30 minutes at 37°C, washed and subsequently processed for immunofluorescence. Fluorescence intensity quantification of each protein and CMFDA staining were performed as described (Nishimura et al., 2004) using the Zeiss Axiovision 4.6 software. As a control, ratiometric analysis was performed for p38, a protein that does not accumulate at axon tips (Gartner et al., 2006). At least 50 cells per condition from a total of three experiments were analyzed.

Statistical analysis was performed using a Kruskal-Wallis nonparametric analysis of variance test and Dunn's post-hoc tests with InStat 3.0 (GraphPad Software).

IP and Ral-GTP pull down assay

After two washes in cold PBS, cells from two 10 cm dishes per condition were scraped in 100 μl of IP buffer containing 150 mM NaCl, 10 mM Tris (pH 7.4), 1 mM EDTA, 1 mM EGTA pH 8.0, 1 mM $MgCl_2$, 1 mM Na_3VO_4, 10 mM NaF, 1 mM PMSF and one Complete protease-inhibitor tablet/10 ml (Roche). After incubating 30 minutes on ice, lysates were cleared by centrifugation at 19,280 × ***g*** for 15 minutes at 4°C and pre-cleared for 1 hour with protein G-Sepharose on a rotating wheel at 4°C. Protein concentration was measured in supernatants using a Bradford assay (Bio-Rad Laboratories). Extracts were then incubated with 2 μg antibody and protein G-Sepharose 4-10 hours at 4°C. After centrifugation for 5 minutes at 560 × ***g*** beads were washed four times with IP buffer containing 250 mM NaCl and 0.5% Triton. Western blot analysis was then performed on cell lysates as described (Lalli and Hall, 2005). Quantification by optical density was performed using NIH ImageJ on four independent experiments. Ral-GTP pull-down assays were performed as described (Lalli and Hall, 2005).

I am very grateful to Alan Hall and Patrick Doherty for their support, and to Martina Sonego for valuable assistance. I thank Enzo Lalli, Giovanni Lesa, Karni Schlessinger and Volker Stucke for helpful comments; Shu Hsu for the anti-Exo84 antibody; and Carl Hobbs and Julian Ng for microscopy help. This work was supported by a King's College Young Investigator Fellowship to G.L.

References

Anitei, M., Ifrim, M., Ewart, M. A., Cowan, A. E., Carson, J. H., Bansal, R. and Pfeiffer, S. E. (2006). A role for Sec8 in oligodendrocyte morphological differentiation. *J. Cell Sci.* **119**, 807-818.

Arimura, N. and Kaibuchi, K. (2007). Neuronal polarity: from extracellular signals to intracellular mechanisms. *Nat. Rev. Neurosci.* **8**, 194-205.

Barnes, A. P., Solecki, D. and Polleux, F. (2008). New insights into the molecular mechanisms specifying neuronal polarity *in vivo*. *Curr. Opin. Neurobiol.* **18**, 44-52.

Blankenship, J. T., Fuller, M. T. and Zallen, J. A. (2007). The Drosophila homolog of the Exo84 exocyst subunit promotes apical epithelial identity. *J. Cell Sci.* **120**, 3099-3110.

Bradke, F. and Dotti, C. G. (1997). Neuronal polarity: vectorial cytoplasmic flow precedes axon formation. *Neuron* **19**, 1175-1186.

Calderon de Anda, F., Gartner, A., Tsai, L. H. and Dotti, C. G. (2008). Pyramidal neuron polarity axis is defined at the bipolar stage. *J. Cell Sci.* **121**, 178-185.

Chen, Y. M., Wang, Q. J., Hu, H. S., Yu, P. C., Zhu, J., Drewes, G., Piwnica-Worms, H. and Luo, Z. G. (2006). Microtubule affinity-regulating kinase 2 functions downstream of the PAR-3/PAR-6/atypical PKC complex in regulating hippocampal neuronal polarity. *Proc. Natl. Acad. Sci. USA* **103**, 8534-8539.

Dajas-Bailador, F., Jones, E. V. and Whitmarsh, A. J. (2008). The JIP1 scaffold protein regulates axonal development in cortical neurons. *Curr. Biol.* **18**, 221-226.

Dotti, C. G., Sullivan, C. A. and Banker, G. A. (1988). The establishment of polarity by hippocampal neurons in culture. *J. Neurosci.* **8**, 1454-1468.

Elbert, M., Rossi, G. and Brennwald, P. (2005). The yeast par-1 homologs kin1 and kin2 show genetic and physical interactions with components of the exocytic machinery. *Mol. Biol. Cell* **16**, 532-549.

Feig, L. A. (2003). Ral-GTPases: approaching their 15 minutes of fame. *Trends Cell Biol.* **13**, 419-425.

Frische, E. W., Pellis-van Berkel, W., van Haaften, G., Cuppen, E., Plasterk, R. H., Tijsterman, M., Bos, J. L. and Zwartkruis, F. J. (2007). RAP-1 and the RAL-1/exocyst pathway coordinate hypodermal cell organization in Caenorhabditis elegans. *EMBO J.* **26**, 5083-5092.

Gartner, A., Huang, X. and Hall, A. (2006). Neuronal polarity is regulated by glycogen synthase kinase-3 (GSK-3beta) independently of Akt/PKB serine phosphorylation. *J. Cell Sci.* **119**, 3927-3934.

Goldstein, B. and Macara, I. G. (2007). The PAR proteins: fundamental players in animal cell polarization. *Dev. Cell* **13**, 609-622.

Grindstaff, K. K., Yeaman, C., Anandasabapathy, N., Hsu, S. C., Rodriguez-Boulan, E., Scheller, R. H. and Nelson, W. J. (1998). Sec6/8 complex is recruited to cell-cell contacts and specifies transport vesicle delivery to the basal-lateral membrane in epithelial cells. *Cell* **93**, 731-740.

Hsu, S. C., Hazuka, C. D., Roth, R., Foletti, D. L., Heuser, J. and Scheller, R. H. (1998). Subunit composition, protein interactions, and structures of the mammalian brain sec6/8 complex and septin filaments. *Neuron* **20**, 1111-1122.

Lalli, G. and Hall, A. (2005). Ral GTPases regulate neurite branching through GAP-43 and the exocyst complex. *J. Cell Biol.* **171**, 857-869.

Langevin, J., Morgan, M. J., Sibarita, J. B., Aresta, S., Murthy, M., Schwarz, T., Camonis, J. and Bellaiche, Y. (2005). Drosophila exocyst components Sec5, Sec6, and Sec15 regulate DE-Cadherin trafficking from recycling endosomes to the plasma membrane. *Dev. Cell* **9**, 355-376.

Mehta, S. Q., Hiesinger, P. R., Beronja, S., Zhai, R. G., Schulze, K. L., Verstreken, P., Cao, Y., Zhou, Y., Tepass, U., Crair, M. C. et al. (2005). Mutations in Drosophila sec15 reveal a function in neuronal targeting for a subset of exocyst components. *Neuron* **46**, 219-232.

Moskalenko, S., Henry, D. O., Rosse, C., Mirey, G., Camonis, J. H. and White, M. A. (2002). The exocyst is a Ral effector complex. *Nat. Cell Biol.* **4**, 66-72.

Moskalenko, S., Tong, C., Rosse, C., Mirey, G., Formstecher, E., Daviet, L., Camonis, J. and White, M. A. (2003). Ral GTPases regulate exocyst assembly through dual subunit interactions. *J. Biol. Chem.* **278**, 51743-51748.

Nishimura, T., Kato, K., Yamaguchi, T., Fukata, Y., Ohno, S. and Kaibuchi, K. (2004). Role of the PAR-3-KIF3 complex in the establishment of neuronal polarity. *Nat. Cell Biol.* **6**, 328-334.

Nishimura, T., Yamaguchi, T., Kato, K., Yoshizawa, M., Nabeshima, Y., Ohno, S., Hoshino, M. and Kaibuchi, K. (2005). PAR-6-PAR-3 mediates Cdc42-induced Rac activation through the Rac GEFs STEF/Tiam1. *Nat. Cell Biol.* **7**, 270-277.

Omidvar, N., Pearn, L., Burnett, A. K. and Darley, R. L. (2006). Ral is both necessary and sufficient for the inhibition of myeloid differentiation mediated by Ras. *Mol. Cell. Biol.* **26**, 3966-3975.

Rosse, C., Hatzoglou, A., Parrini, M. C., White, M. A., Chavrier, P. and Camonis, J. (2006). RalB mobilizes the exocyst to drive cell migration. *Mol. Cell. Biol.* **26**, 727-734.

Sans, N., Prybylowski, K., Petralia, R. S., Chang, K., Wang, Y. X., Racca, C., Vicini, S. and Wenthold, R. J. (2003). NMDA receptor trafficking through an interaction between PDZ proteins and the exocyst complex. *Nat. Cell Biol.* **5**, 520-530.

Schwamborn, J. C. and Puschel, A. W. (2004). The sequential activity of the GTPases Rap1B and Cdc42 determines neuronal polarity. *Nat. Neurosci.* **7**, 923-929.

Schwamborn, J. C., Khazaei, M. R. and Puschel, A. W. (2007). The interaction of mPar3 with the ubiquitin ligase Smurf2 is required for the establishment of neuronal polarity. *J. Biol. Chem.* **282**, 35259-35268.

Spiczka, K. S. and Yeaman, C. (2008). Ral-regulated interaction between Sec5 and paxillin targets Exocyst to focal complexes during cell migration. *J. Cell Sci.* **121**, 2880-2891.

Sugihara, K., Asano, S., Tanaka, K., Iwamatsu, A., Okawa, K. and Ohta, Y. (2002). The exocyst complex binds the small GTPase RalA to mediate filopodia formation. *Nat. Cell Biol.* **4**, 73-78.

Tian, X., Rusanescu, G., Hou, W., Schaffhausen, B. and Feig, L. A. (2002). PDK1 mediates growth factor-induced Ral-GEF activation by a kinase-independent mechanism. *EMBO J.* **21**, 1327-1338.

Vega, I. E. and Hsu, S. C. (2001). The exocyst complex associates with microtubules to mediate vesicle targeting and neurite outgrowth. *J. Neurosci.* **21**, 3839-3848.

Ward, Y., Wang, W., Woodhouse, E., Linnoila, I., Liotta, L. and Kelly, K. (2001). Signal pathways which promote invasion and metastasis: critical and distinct contributions of extracellular signal-regulated kinase and Ral-specific guanine exchange factor pathways. *Mol. Cell. Biol.* **21**, 5958-5969.

Wu, S., Mehta, S. Q., Pichaud, F., Bellen, H. J. and Quiocho, F. A. (2005). Sec15 interacts with Rab11 via a novel domain and affects Rab11 localization *in vivo*. *Nat. Struct. Mol. Biol.* **12**, 879-885.

Zhang, X., Zajac, A., Zhang, J., Wang, P., Li, M., Murray, J., TerBush, D. and Guo, W. (2005). The critical role of Exo84p in the organization and polarized localization of the exocyst complex. *J. Biol. Chem.* **280**, 20356-20364.

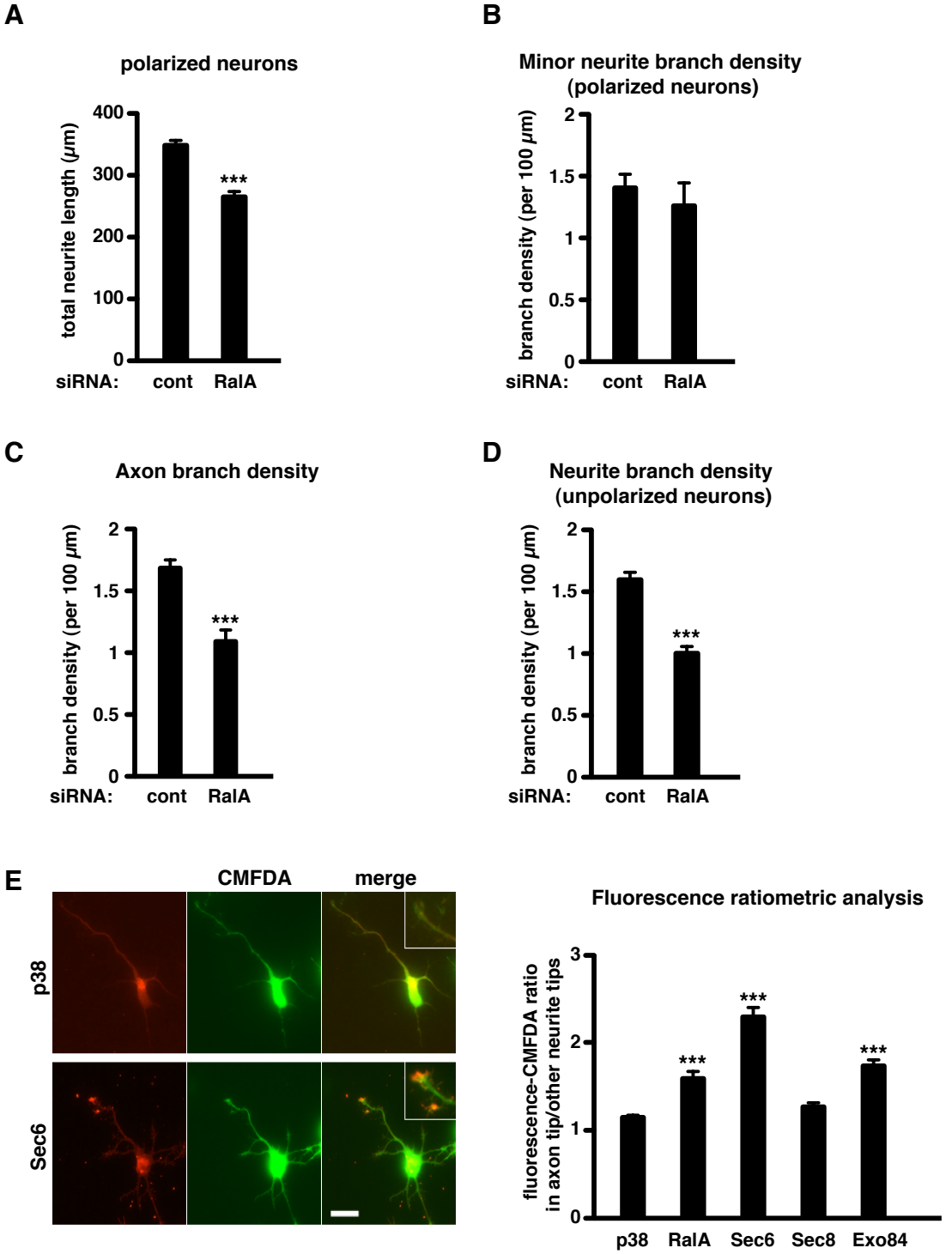
A
polarized neurons
total neurite length (μm)
400
300
200
100
0
***
siRNA: cont RalA
B
Minor neurite branch density
(polarized neurons)
branch density (per 100 μm)
2
1.5
1
0.5
0
siRNA: cont RalA
C
Axon branch density
branch density (per 100 μm)
2
1.5
1
0.5
0
***
siRNA: cont RalA
D
Neurite branch density
(unpolarized neurons)
branch density (per 100 μm)
2
1.5
1
0.5
0
***
siRNA: cont RalA
E
CMFDA
merge
p38
Sec6
Fluorescence ratiometric analysis
fluorescence-CMFDA ratio
in axon tip/other neurite tips
3
2
1
0
***
***
***
p38 RalA Sec6 Sec8 Exo84

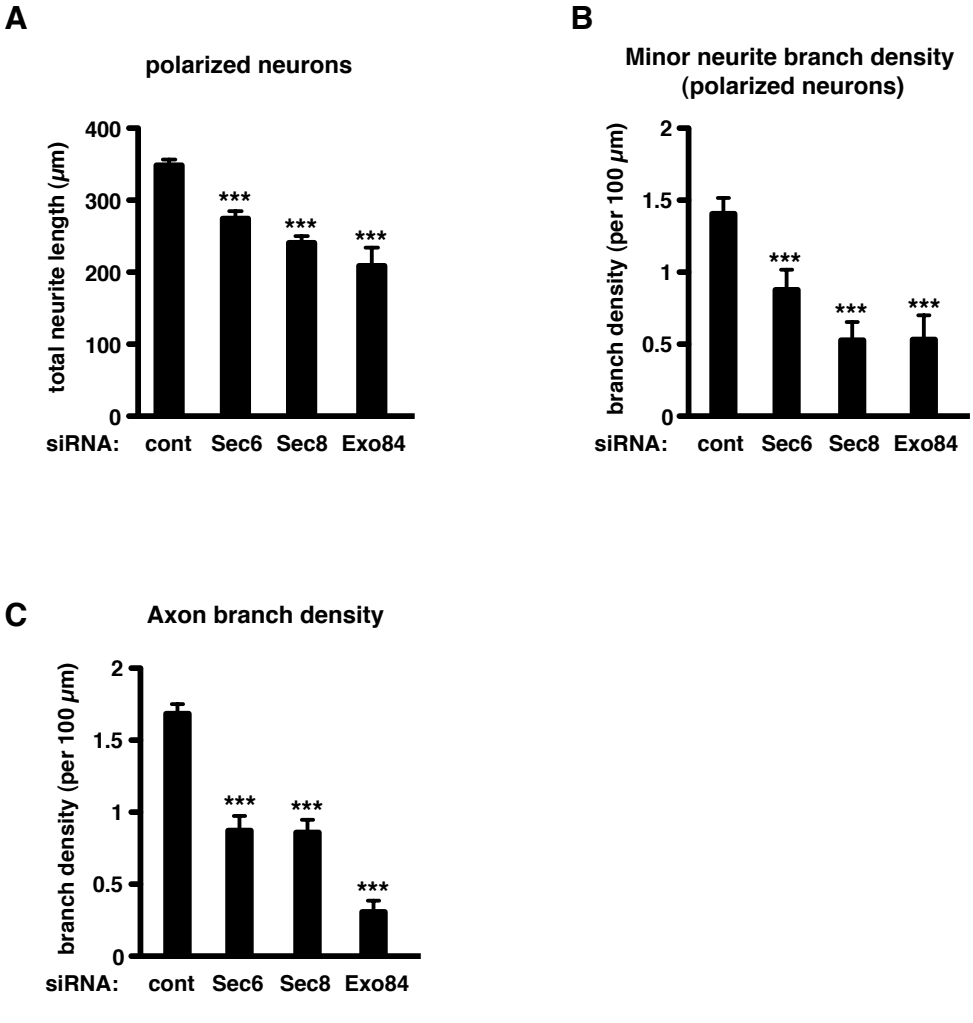
A
polarized neurons
total neurite length (μm)
400
300
200
100
0
***
***
***
siRNA:
cont
Sec6
Sec8
Exo84
B
Minor neurite branch density
(polarized neurons)
branch density (per 100 μm)
2
1.5
1
0.5
0
***
***
***
siRNA:
cont
Sec6
Sec8
Exo84
C
Axon branch density
branch density (per 100 μm)
2
1.5
1
0.5
0
***
***
***
siRNA:
cont
Sec6
Sec8
Exo84

siRNA: cont RalA WB:

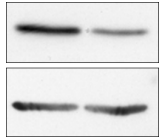

RalA

β-actin

siRNA: cont Sec6 WB:

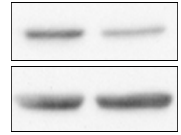

Sec6

β-actin

siRNA: cont Sec8 WB:

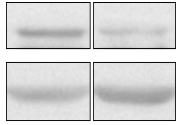

Sec8

β-actin

siRNA: cont Exo84 WB:

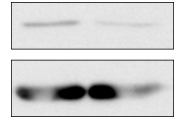

Exo84

β-actin